Journal of proteome research

Article

pubs.acs.org/jpr

Comparative Proteomic and Metabolomic Analysis of *Staphylococcus warneri* SG1 Cultured in the Presence and Absence of Butanol

Feifei Fu,[†] Victor W. T. Cheng,[‡] Yiman Wu,[†] Yanan Tang,[†] Joel H. Weiner,*[,‡] and Liang Li*[,†]

[†]Department of Chemistry and [‡]Department of Biochemistry, University of Alberta, Edmonton, Alberta T6G2G2, Canada

Supporting Information

ABSTRACT: The complete genome of the solvent tolerant *Staphylococcus warneri* SG1 was recently published. This Gram-positive bacterium is tolerant to a large spectrum of organic solvents including short-chain alcohols, alkanes, esters and cyclic aromatic compounds. In this study, we applied a two-dimensional liquid chromatography (2D-LC) mass spectrometry (MS) shotgun approach, in combination with quantitative 2-MEGA (dimethylation after guanidination) isotopic labeling, to compare the proteomes of SG1 grown under butanol-free and butanol-challenged conditions. In total, 1585 unique proteins (representing 65% of the predicted open reading frames) were identified, covering all major metabolic pathways. Of the 967 quantifiable proteins by 2-MEGA labeling, 260 were differentially expressed by at least 1.5-fold. These proteins are involved in energy metabolism, oxidative stress response, lipid and cell envelope biogenesis, or have chaperone functions. We also applied differential isotope labeling LC-MS to probe metabolite changes in key metabolic pathways upon butanol stress. This is the first comprehensive proteomic and metabolomic study of *S. warneri* SG1 and presents an important step toward understanding its physiology and mechanism of solvent tolerance.

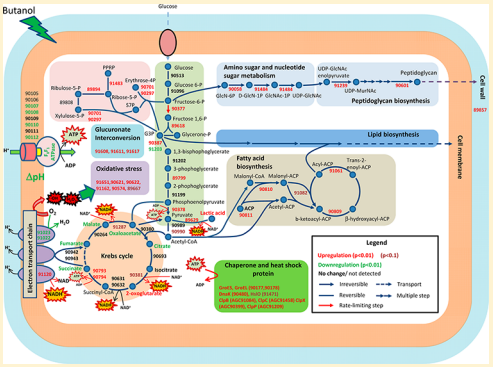

KEYWORDS: *Staphylococcus warneri SG1, bacterium, butanol, quantitative proteomics, quantitative metabolomics, solvent tolerance*

INTRODUCTION

Engineering solvent tolerant microorganisms for biodegradation, biofuel production, and biocatalysis of high value compounds is an important branch of synthetic biology. However, these endeavors are often hindered by the toxicity of organic compounds, which damage important macromolecules such as DNA, RNA, and proteins, as well as disrupt biological membrane functions such as transport and cause dissipation of the proton motive force. Adaptation of the bacterium to survive in a high titer of organic solvent is achieved through global changes that include alteration of the membrane structure and fluidity, differential protein expression, and activation of specific defense mechanisms. The interplay between solvent stress and cellular response is thoroughly reviewed.[1−6] In spite of this, the fact that solvent tolerant bacteria isolated, either selectively or naturally, outnumbers those with acquired tolerance via targeted genetic manipulation is a testament of the complexity and multifacet nature of how microorganisms cope with solvent stress.

In general, Gram-negative bacteria have a higher tolerance against organic solvents because they have an additional outer membrane and thus are more widely studied compared to Gram-positive bacteria.[3] In recent years, the number of solvent tolerant Gram-positive bacteria isolated and studied has increased, especially those from the *Staphylococcus* and *Bacillus* genera.[7−10] *Staphylococcus warneri* is a solvent tolerant Gram-positive bacterium that constitutes a part of the human skin flora, and its genome was recently published.[11] The genome consists of 2.56 Mbases and is estimated to encode 2457 open reading frames. This bacterium, specifically the SG1 strain, is tolerant to alkanes, short-chain alcohols, esters, and cyclic aromatic compounds; in particular, SG1 could grow in the presence of 2.5% 1-butanol, making it an excellent candidate chassis for biofuel production.

Classical fermentation of *Clostridium acetobutylicum* on molasses or grains yields acetone, butanol, and ethanol.[12] With the advent of synthetic biology, notably in *Escherichia coli* and *Saccharomyces cerevisiae*, novel or heterologous metabolic pathways can be engineered to produce butanol and numerous high value chemicals.[13−16] However, butanol titers from these biological systems are believed to be limited by the chaotropic effects of the end product. A number of studies on the aforementioned model organisms have attempted to elucidate the complex mechanism of solvent tolerance using genomics, proteomics, and metabolomics discovery approaches.[17−21] Though informative, the shotgun proteomic approach identified only a small subset of predicted proteins using *C. acetobutylicum*[20,21] and *Pseudomonas putida*[22,23] as query organisms.

In this study, we first applied two-dimensional liquid chromatography (2D-LC) tandem mass spectrometry (MS/MS) (2D-LC−MS/MS) profiling of the whole cell lysates and established a reference map covering 65% of the predicted

Received: June 6, 2013
Published: August 20, 2013

dx.doi.org/10.1021/pr400533m | J. Proteome Res. 2013, 12, 4478−4489

proteome. We then employed 2-MEGA labeling to carry out comparative proteomic analysis of SG1 grown in the presence ($BtOH^+$) and absence ($BtOH^-$) of butanol using 2D-LC−MS/MS. Of the 967 quantified proteins, we found proteins involved in energy metabolism, lipid and cell envelope biogenesis, and those with chaperone functions to be differentially up-regulated. Finally we used an isotope labeling LC−MS method to investigate the metabolomic changes of SG1 upon butanol exposure. The combination of proteomic and metabolomic data provides detailed insight into the solvent tolerance mechanism of SG1.

EXPERIMENTAL SECTION

Chemicals and Reagents

All the chemicals and reagents, unless otherwise stated, were purchased from Sigma-Aldrich Canada (Markham, ON, Canada). Lysostaphin was purchased from AMBI Products (Lawrence, NY). Isotopically enriched reagents including formaldehyde ($^{13}CD_2O$) were purchased from Cambridge Isotope Laboratories (Andover, MA). For dansylation and *p*-dimethylaminophenacyl (DmPA) labeling reactions, the ^{12}C-labeling reagents without depletion of ^{13}C isotopes were from Sigma-Aldrich, where the ^{13}C-labeling reagents were synthesized in our lab using the procedures published previously.[24,25] Phosphoric acid (H_3PO_4), potassium chloride (KCl), potassium dihydrogen phosphate (KH_2PO_4), and ammonium bicarbonate (NH_4HCO_3) were purchased from EMD Chemical, Inc. (Mississauga, ON, Canada). Sequencing grade modified trypsin, HPLC grade formic acid, LC−MS grade water, acetone, and acetonitrile (ACN) were purchased from Fisher Scientific Canada (Edmonton, AB, Canada). A domestic 900 W (2450 MHz) sunbeam microwave oven was used to perform microwave-assisted protein solubilization experiments.

Cell Growth and Protein Sample Preparation

Cultures of *S. warneri* strain SG1 were routinely grown in Luria−Bertani broth at 37 °C with shaking for 16 h. For MS studies, 2 L cultures were grown in triplicate (seeded with a 0.1% inoculum), with or without 1.5% (v/v) 1-butanol, and harvested by centrifugation at 8000 × *g* for 15 min and resuspended in 100 mM Tris/5 mM EDTA buffer, pH 7.0. Cell lysis was carried out either mechanically by repeated passage (4×) through a Constant Systems TS benchtop cell disruptor (Daventry, Northants., U.K.) at 40 kpsi, or enzymatically by adding NaCl (100 mM), lysostaphin (10 μg mL^{-1}), and lysozyme (50 μg mL^{-1}), followed by incubation at 37 °C for 1 h. Unbroken cells and cell debris were removed by centrifugation at 10 000 × *g* for 20 min, and the cell lysates were frozen immediately with liquid nitrogen.

Protein assays were performed to adjust protein concentrations of lysates to similar levels. Acetone, precooled to −80 °C, was gradually added to the whole cell lysates to a final concentration of 80% (v/v), and the mixtures were incubated overnight at −80 °C. Samples were then spun at 20 800 × *g* for 20 min, and the pellets were washed with 40 μL of prechilled acetone before drying at room temperature. The pellets were then subjected to microwave-assisted protein solubilization in urea.[26] Briefly, 8 M urea was added to the whole cell lysates followed by six cycles of microwave irradiation in 30 s cycles with sample cooling and homogenization between cycles. The mixtures were then centrifuged at 20 800 × *g* for 5 min, and the pellets were subjected to a fresh round of microwave-assisted protein solubilization. Upon complete solubilization of the pellets, the supernatant fractions were pooled and diluted with 100 mM NH_4HCO_3 to reduce the urea concentration to ∼1 M. Samples were analyzed by protein assay and reduced with dithiothreitol for 1 h at 37 °C, followed by alkylation with iodoacetamide for 0.5 h at room temperature in the dark. Trypsin was added to a protein/trypsin ratio of 40:1 and incubated at 37 °C for 20 h for complete digestion. The tryptic digests were acidified with 50% trifluoroacetic acid to pH 2 and injected into an Agilent 1100 HPLC system (Palo Alto, CA) for desalting and quantification. A Polaris C18-A column (4.6 mm × 50 mm, 3 μm particle size, 300 Å pore size) (Varian, Palo Alto, CA) was used for desalting, and a UV detector operating at 214 nm was used for quantification of the eluted peptides.[27]

Proteome Profiling

2D-LC-MS/MS was used for generating a qualitative profile of the SG1 proteome. After protein digestion, the desalted peptides were dried, reconstituted in 0.2% H_3PO_4 (pH 2.0), and separated by SCX liquid chromatography using a polysulfoethyl A column (2.1 mm × 250 mm, 5 μm particle size, 300 Å pore size) (PolyLC, Columbia, MD). Peptides were fractionated using the following gradient: mobile phases A (10 mM KH_2PO_4, pH 2.76) and B (10 mM KH_2PO_4, pH 2.76, 500 mM KCl); t = 0 min, 0% B; t = 1 min, 4% B; t = 17 min, 20% B; t = 39 min, 60% B; t = 45 min, 100% B; t = 50 min, 100% B; t = 52 min, 0% B; t = 62 min, 0% B. The collected peptide fractions were then desalted and quantified. Less abundant neighbor fractions were combined to a total of 20 fractions.

The SCX fractionated peptides were further separated by reversed phase liquid chromatography (RPLC) using a nanoACQUITY UltraPerformance LC system (Waters, Missisauga, ON) with an Atlantis dC18 column (75 μm × 150 mm, 3 μm particle size, 100 Å pore size) (Waters, Milford, MA). The following gradient was applied to separate the peptides: mobile phase A (0.1% FA in water) and B (0.1% FA in ACN); t = 0 min, 2% B; t = 2 min, 7% B; t = 85 min, 20% B; t = 105 min, 30% B; t = 110 min, 45% B; t = 120 min, 90% B; t = 125 min, 90% B; t = 130 min, 95% B.[27] The eluted peptides were then electrosprayed into an electrospray ionization (ESI) quadrupole time-of-flight (Q-TOF) premier mass spectrometer (Waters, Missisauga, ON) at a flow rate of 350 nL min^{-1}. A survey MS scan was acquired from m/z 350−1600 for 0.8 s, followed by eight data-dependent MS/MS scans. A mass tolerance window of 80 mDa was applied for both dynamic and precursor ion exclusion,[28] with a retention time tolerance window of 150 s. The collision energy used for MS/MS analysis was varied based on the precursor ion mass and charge state. A mixture of leucine enkephalin and (Glu1)-fibrinopeptide B, used as mass calibrants (i.e., lock-mass), was infused at a flow rate of 300 nL min^{-1}, and a 1 s MS scan was acquired every 1 min throughout the run. Each SCX fraction was analyzed twice on the RPLC-MS with a precursor ion exclusion list involved in each of the second run to eliminate redundant identification.

Raw RPLC-MS data were lock-mass corrected, de-isotoped, and converted to peak list files with retention time information using the ProteinLynx Global Server 2.3.0. The peak list files were processed using MASCOT (Matrix Science, London, U.K. version 2.2.1) to attain peptide sequence information. Database search was restricted to the 2457 predicted open reading frames from SG1. The search parameters were selected as follows: enzyme, trypsin; missed cleavages, 1; peptide tolerance, 30 ppm; MS/MS tolerance, 0.2 Da; peptide charge, (+1, +2, and +3); fixed modification, carbamidomethylation (C); variable

dx.doi.org/10.1021/pr400533m | J. Proteome Res. 2013, 12, 4478−4489

modifications, oxidation (M) and carbamylation (N-term). Identified peptides with scores larger than the MASCOT threshold score at a 95% confidence level were retained to generate the final $BtOH^-$ and $BtOH^+$ proteomes.

The false positive peptide matching rate of our analysis was gauged by the target-decoy searching strategy.[29] Semiquantitative analysis of identified proteins was determined by the exponentially modified protein abundance index (emPAI value) based on protein coverage by the peptide matches in a database search result. The emPAI values obtained from the MASCOT server were normalized using the following equation.[30]

$$\text{normalized emPAI} = \frac{\text{emPAI}_{\text{protein}}}{\text{emPAI}_{\text{total}}} \times 100\%$$

Quantification of Proteome Changes Using 2-MEGA Labeling and LC-MS

2-MEGA isotopic labeling was carried out on biological triplicate of SG1 grown in the absence and presence of BtOH according to the workflow shown in Supporting Information Figure S1. After protein digestion, the $BtOH^-$ and $BtOH^+$ peptides were individually labeled with either heavy chain or light chain using the 2-MEGA labeling method.[31−33] Briefly, 4 M *O*-methylisourea was added to the peptide mixtures and the pH was adjusted to 11 with 2 M NaOH. Samples were incubated at 60 °C for 20 min with intermittent shaking to guanidinate the lysine side chains. The pH was then adjusted to 6 using 50% trifluoroacetic acid and further adjusted to 4.5 using acetate buffer. Then 1 M $NaCNBH_3$ and 4% formaldehyde ($^{12}CH_2O$ for light chain labeling and $^{13}CD_2O$ for heavy chain labeling) were added to dimethylate the N-termini of the peptides. After labeling, a small amount of 1 M NH_4HCO_3 was added to consume the excess formaldehyde and the reaction was quenched by adjusting the pH to 2 using 10% trifluoroacetic acid. Finally, labeled peptides were desalted and quantified. Heavy chain labeled $BtOH^-_H$ was mixed with light chain labeled $BtOH^+_L$ in a 1:1 ratio based on the total peptide content by weight as forward labeling. Similarly, reverse labeling was done by mixing light chain labeled $BtOH^-_L$ with heavy chain labeled $BtOH^+_H$. The $BtOH^-_L$:$BtOH^+_H$ and $BtOH^+_L$:$BtOH^-_H$ mixtures were analyzed by 2D-LC−MS/MS as described above with the exception that each SCX fraction was only analyzed once and a survey MS scan was followed by four data-dependent MS/MS scans.

Raw MS and MS/MS data were searched using MASCOT DISTILLER with the following parameters: taxonomy, all entries; enzyme, trypsin; missed cleavages, 1; fixed modifications, carbamidomethylation (C) and guanidination (K); variable modifications, dimethylation d_0 ($+^{12}C_2H_4$, +28.0313 Da, N-term), dimethylation d_6 ($+^{13}C_2D_4$, +34.0631 Da, N-term), Oxidation (M); peptide tolerance, 30 ppm; MS/MS tolerance, 0.2 Da. A modified ESI-Q-TOF ion fragmentation series that permitted a-type ions was applied. The relative intensity ratios for peak pairs were extracted and normalized using the median ratios to avoid system bias. In cases where same peptide pairs were detected multiple times in different SCX fractions or where peptide pairs with same sequences but different charge states, the relative ratios of the peptides pairs were averaged. Peptides with relative error > 1 in forward and reverse labeling were discarded. Protein ratios were calculated based on the geometric mean of peptide ratios from the same protein. Finally, six lists of protein ratios were generated from the biological triplicate samples (each sample set contains a pair of forward and reverse labeling data). To identify differentially expressed proteins with statistical confidence, the following procedures were used. First, proteins quantified in less than two biological samples were discarded. The geometric mean of protein ratios from different replicates were calculated and subjected to one-sample *t*-test where only proteins with $p < 0.01$ were retained,[34,35] followed by applying a 1.5-fold cutoff threshold for differential expression. Global protein expression profiles were analyzed by Cluster of Orthologous Groups (COG)[36] and the Kyoto Encyclopedia of Genes and Genomes (KEGG) server.[37]

Quantification of Metabolome Changes Using Isotope Labeling LC−MS

For metabolite extraction, whole cell lysates from $BtOH^-$ and $BtOH^+$ cells were prepared as described above. A volume of 1200 μL of acetone was added to 300 μL of the whole cell lysates to precipitate the proteins. The supernatants were dried using a SpeedVac and resuspended in either 50 μL of water for dansylation labeling or 90 μL of water for *p*-dimethylaminophenacyl (DmPA) labeling.

For dansylation labeling, the 50 μL solution was mixed with 25 μL of 250 mM sodium carbonate/sodium bicarbonate buffer and ACN, vortexed, spun down, and mixed with 50 μL of freshly prepared ^{12}C-dansyl chloride solution (18 mg mL^{-1}) (light labeling) or ^{13}C-dansyl chloride solution (18 mg mL^{-1}) (heavy labeling). The reaction was allowed to proceed for 1 h at 60 °C, followed by addition of 10 μL of 250 mM NaOH to quench the excess dansyl chloride. The solution was then incubated at 60 °C for another 10 min. Finally, 50 μL of 425 mM formic acid in 1:1 ACN/H_2O was added to consume the excess NaOH and to acidify the solution.

For DmPA labeling, 90 μL of solution was first acidified with HCl and extracted with 300 μL of ethyl acetate. The organic layer was dried and dissolved in 60 μL of 20 mg mL^{-1} triethylamine, and then mixed with 60 μL of freshly prepared ^{12}C-DmPA bromide solution (20 mg mL^{-1}) (light labeling) or ^{13}C-DmPA bromide solution (20 mg mL^{-1}) (heavy labeling). The reaction was allowed to proceed for 50 min at 90 °C and quenched with 50 μL of 20 mg mL^{-1} triphenylacetic acid for 30 min at 90 °C.

An LC-UV quantification step was carried out prior to mass analysis in order to control the amount of sample used for metabolome comparison.[38] A volume of 2 μL of the labeled solution was injected onto a Phenomenex C18 column (2.1 mm × 5 cm, 1.7 μm particle size, 100 Å pore size). For amine quantification, the gradient started with 100% A (0.1% (v/v) formic acid in 5% (v/v) ACN) and 0% B (0.1% (v/v) formic acid in ACN) for 1 min and was changed to 5% A/95% B within 0.01 min and held for 1 min. The gradient was restored to 100% A/0% B in 0.5 min and held for 3.5 min to re-equilibrate the column. For acid quantitation, the gradient started with 20% B for 2 min and was increased to 85% B within 0.01 min and held for 2 min and then increased to 95% B within 0.01 min and held at 95% B for 1 min. The gradient was restored back to 20% B in 1 min and held for 3 min to re-equilibrate the column. The flow rate was 450 μL min^{-1}.

The labeled metabolites were analyzed using a Bruker 9.4 T Apex-Qe Fourier transform ion-cyclotron resonance (FTICR) mass spectrometer (Bruker, Billerica, MA) linked to an Agilent 1100 series binary HPLC system (Agilent, Palo Alto, CA). The samples were injected onto an Agilent RP Eclipse Plus C18 column (2.1 mm × 10 cm, 1.8 μm particle size, 95 Å pore size)

dx.doi.org/10.1021/pr400533m | J. Proteome Res. 2013, 12, 4478−4489

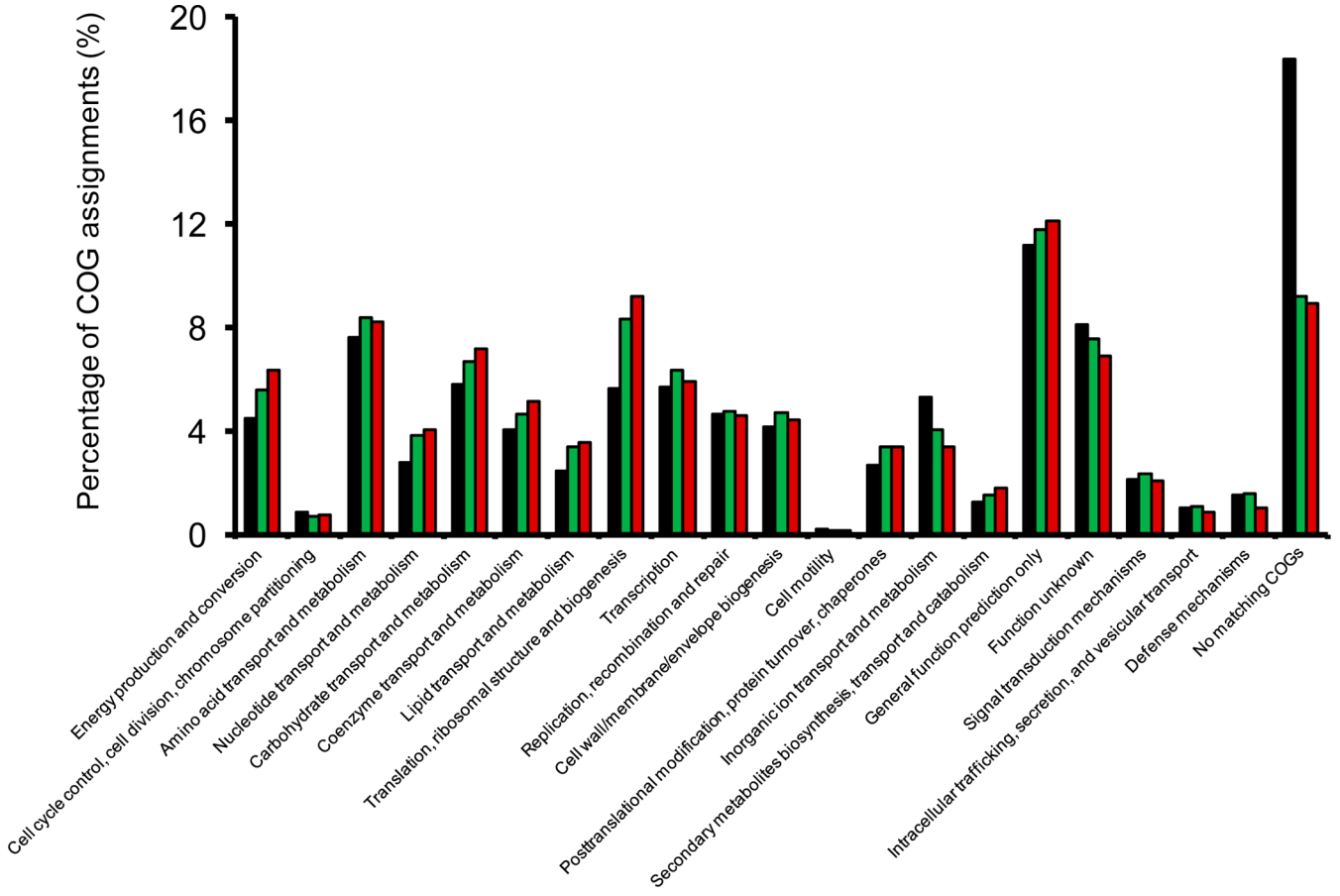

Figure 1. Percentage distribution of proteins by cluster of orthologous groups showing the predicted (black), $BtOH^-$ (green), and $BtOH^+$ (red) proteomes of *S. warneri* SG1.

for separation. Solvent A was 0.1% (v/v) formic acid in 5% (v/v) ACN, and solvent B was 0.1% (v/v) formic acid in ACN. The chromatographic conditions for amine labeling were t = 0 min, 20% B; t = 3.5 min, 35% B; t = 18 min, 65% B; t = 21 min, 95% B; t = 26 min, 95% B. The gradient for acid labeling was t = 0 min, 20% B; t = 9 min, 50% B; t = 22 min, 65% B; t = 26 min, 80% B; t = 29 min, 98% B; t = 30 min, 98% B. The flow rate was 180 μL min^{-1}. All MS spectra were obtained in the positive ion mode. The resulting MS data were processed using R language program based on XCMS[39] written specifically for $^{12}C/^{13}C$ peak pair picking.[40] This program eliminated the false positive peaks, such as isotopic peaks, common adduct ions, and multiple charged ions. Only the protonated ion pairs were exported for further analysis.

RESULTS AND DISCUSSION

The complete genome sequence of a solvent tolerant Gram-positive bacterium, *S. warneri* strain SG1, was recently published.[11] This bacterium can thrive in the presence of short-chain alcohols, alkanes, esters, and cyclic aromatic compounds, as shown in Supporting Information Table S1. In order to investigate the molecular mechanisms activated or repressed upon butanol challenge, we adopted a mass spectrometry approach to study the proteome of SG1 grown in the absence ($BtOH^-$) and presence ($BtOH^+$) of 1.5% butanol, a concentration which decreased cell yield at stationary phase by approximately 15%. An advantage of this study is that *S. warneri* SG1 boasts a relatively compact proteome comprising 2457 proteins, which is considerably smaller than those of *P. putida*[22,23] (around 5520 proteins) and *C. acetobutylicum*[20,21,41] (around 3850 protein encoding genes) examined in similar studies.

Proteome Profiling and Quantification

In our initial 2D-LC–MS/MS profiling experiments, 8521 and 7944 unique peptides, corresponding to 1477 and 1328 proteins, with a false discovery rate of 1.37% and 1.22%, were identified under $BtOH^-$ and $BtOH^+$ conditions, respectively. A total of 1220 common proteins were detected, while 257 unique proteins were observed only in the absence of butanol and 108 unique proteins were observed in the presence of butanol. In total, 1585 proteins were identified, representing almost 65% of the predicted proteome and in parity with recent MS studies on *Staphylococci* species.[42,43] Supporting Information Table S2 lists the identified proteins in the $BtOH^-$ and $BtOH^+$ proteomes, while Supporting Information Table S3 shows the most abundant proteins that were mapped by 2D-LC–MS/MS. Proteins with one peptide-spectrum match were also included in this list, as our data were acquired using the QTOF instrument and we have demonstrated the reliability of QTOF data for spectrum-to-sequence assignment using sequence database searching.[31]

We first categorized the protein expression profiles by cluster of orthologous groups (COG).[44] The predicted and observed proteomes of SG1 were grouped into 20 functional categories, as shown in Figure 1. The predicted proteome is composed largely (~40%) of proteins which have unknown function (COG class S), have general function prediction only (COG

dx.doi.org/10.1021/pr400533m | J. Proteome Res. 2013, 12, 4478–4489

class R), or have no matching COGs (COG class X). Similarly, large portions (~30%) of both the $BtOH^-$ and $BtOH^+$ proteomes fall into these categories. Excluding these three COG classes, a large number of the observed proteins fall into COG classes J, E, and G, which correspond to protein synthesis, amino acid transport/metabolism, and carbohydrate transport/metabolism, respectively. Comparison of the $BtOH^-$ and $BtOH^+$ proteomes shows that their COG distribution profiles are highly similar (Figure 1) which is consistent with the transcriptome result of butanol stress on *E. coli*.[45] Detailed analyses of metabolic pathways using the Kyoto Encyclopedia of Genes and Genomes (KEGG) database revealed that the enzymes involved in central metabolic pathways such as glycolysis, the tricarboxylic acid cycle, and pentose phosphate pathway were all expressed under both $BtOH^-$ and $BtOH^+$ conditions.

With a proteome reference map in hand, we employed 2-MEGA labeling, followed by 2D-LC−MS/MS, to measure changes in protein expression in SG1 upon butanol challenge. A final list of peptide pairs from both forward and reverse labeling experiments was generated. By discarding outlier data with relative error larger than 1, very good correlation was observed in a $\log_2$–$\log_2$ plot (Supporting Information Figure S2), indicating good analytical reproducibility between the forward and reverse labeling experiments. Data from six independent labeling experiments of biological triplicates were then integrated to give a total of 967 quantified proteins using 2-MEGA labeling. After employing a double-filter, 156 and 104 proteins were identified to be up-regulated or down-regulated at least 1.5-fold, respectively, with *p*-values smaller than 0.01 (Figure 2A; Supporting Information Table S4). The global cellular changes in SG1 upon butanol challenge are represented by Figure 2B. In a $BtOH^+$ environment, proteins in COG classes G (carbohydrate transport and metabolism), O (post-translational modification/protein turnover/chaperones), L (replication, recombination and repair), E (amino acid transport and metabolism), I (lipid transport and metabolism), and M (cell wall/membrane biogenesis) tended to be up-regulated and accounted for more than 50% of the 156 up-regulated proteins. On the other hand, proteins in COG classes P (inorganic ion transport and metabolism), K (transcription), and J (translation) were negatively correlated with butanol exposure.

Metabolic Pathways of SG1 Involved in Butanol Adaptation

The quantitative proteomic analysis of *S. warneri* SG1 enables us to identify important metabolic pathways that are regulated by SG1 upon butanol challenge. Based on the KEGG pathway database, we reconstructed a metabolic pathway map of SG1 for butanol adaption including pathways of glycolysis, Krebs cycle, pentose phosphate pathway, fatty acid biosynthesis, amino sugar and nucleotide sugar metabolism, peptidoglycan biosynthesis, and oxidative phosphorylation (Figure 3). Proteins that have chaperone functions, responsible for oxidative stress response or glucuronate interconversion, were also summarized. The reconstructed pathway map (Figure 3) depicts the dynamic responses of *S. warneri* SG1 upon exposure to 1.5% butanol and illustrates a complicated mechanism for butanol adaptation.

Membrane and Membrane Composition

The first line of defense against solvent exposure is the cell envelope/membrane. An unusual extracellular capsule for *S.*

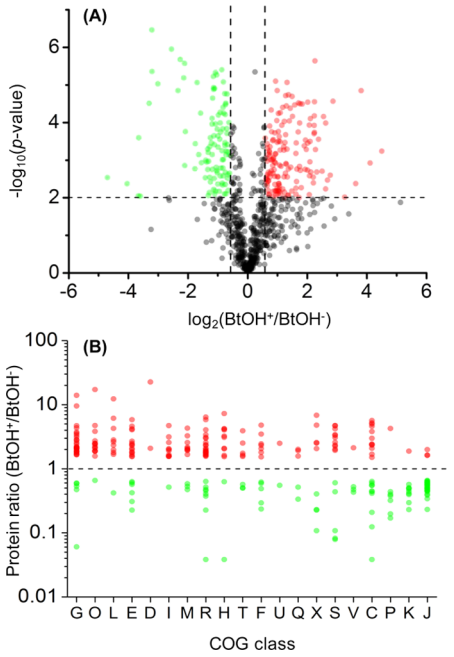

Figure 2. (A) Volcano plot representing changes in protein expression levels upon butanol challenge of *S. warneri* SG1. Differentially expressed proteins that were up-regulated or down-regulated by at least 1.5-fold, with *p*-values smaller than 0.01, are marked in red and green, respectively. (B) Distribution of differentially expressed proteins by cluster of orthologous groups. The COG classes were organized from the most up-regulated class to the most down-regulated class from left to right. COG groups: C, energy production and conversion; D, cell cycle control, cell division, and chromosome partitioning; E, amino acid transport and metabolism; F, nucleotide transport and metabolism; G, carbohydrate transport and metabolism; H, coenzyme transport and metabolism; I, lipid transport and metabolism; J, translation, ribosomal structure, and biogenesis; K, transcription; L, replication, recombination, and repair; M, cell wall/membrane/envelope biogenesis; O, posttranslational modification, protein turnover, and chaperones; P, inorganic ion transport and metabolism; Q, secondary metabolites biosynthesis, transport, and catabolism; R, general function prediction only; S, function unknown; T, signal transduction mechanisms; U, intracellular trafficking, secretion, and vesicular transport; V, defense mechanisms; X, no matching COG.

warneri ZZ1 was developed upon toluene exposure.[8] In our studies, we observed that $BtOH^+$ SG1 cells were resistant to chemical lysis by lysostaphin. Since lysostaphin is a glycylglycine endopeptidase that hydrolyzes the cross-bridges in the peptidoglycan layers of *Staphyloccocci*,[46,47] we can infer that butanol exposure resulted in alteration of the peptidoglycan structure/composition in SG1. In our 2D-LC−MS/MS studies, we observed a larger than 1.5-fold increase in the abundances of UDP-*N*-acetylglucosamine diphosphorylase (AGC91484), UDP-*N*-acetylenolpyruvoylglucosamine reductase (AGC91239), phosphoglucosamine mutase (AGC90058), epimerases (AGC89781, AGC91420, and AGC90069), glycosyltransferases (AGC89738 and AGC91519), penicillin-binding protein 2 (AGC90601), and teichoic acid biosynthesis protein F (AGC89857) (Figure 3, Supporting Information Table S4). These proteins are crucial for the biosynthesis of the peptidoglycan precursors *N*-acetylglucosamine and *N*-acetylmuramic acid, as well as catalyzing their cross-linking via a short polypeptide.[48,49] Meanwhile, the increased amount of teichoic acid synthesized would allow additional modification of the peptidoglycan layer

dx.doi.org/10.1021/pr400533m | J. Proteome Res. 2013, 12, 4478−4489

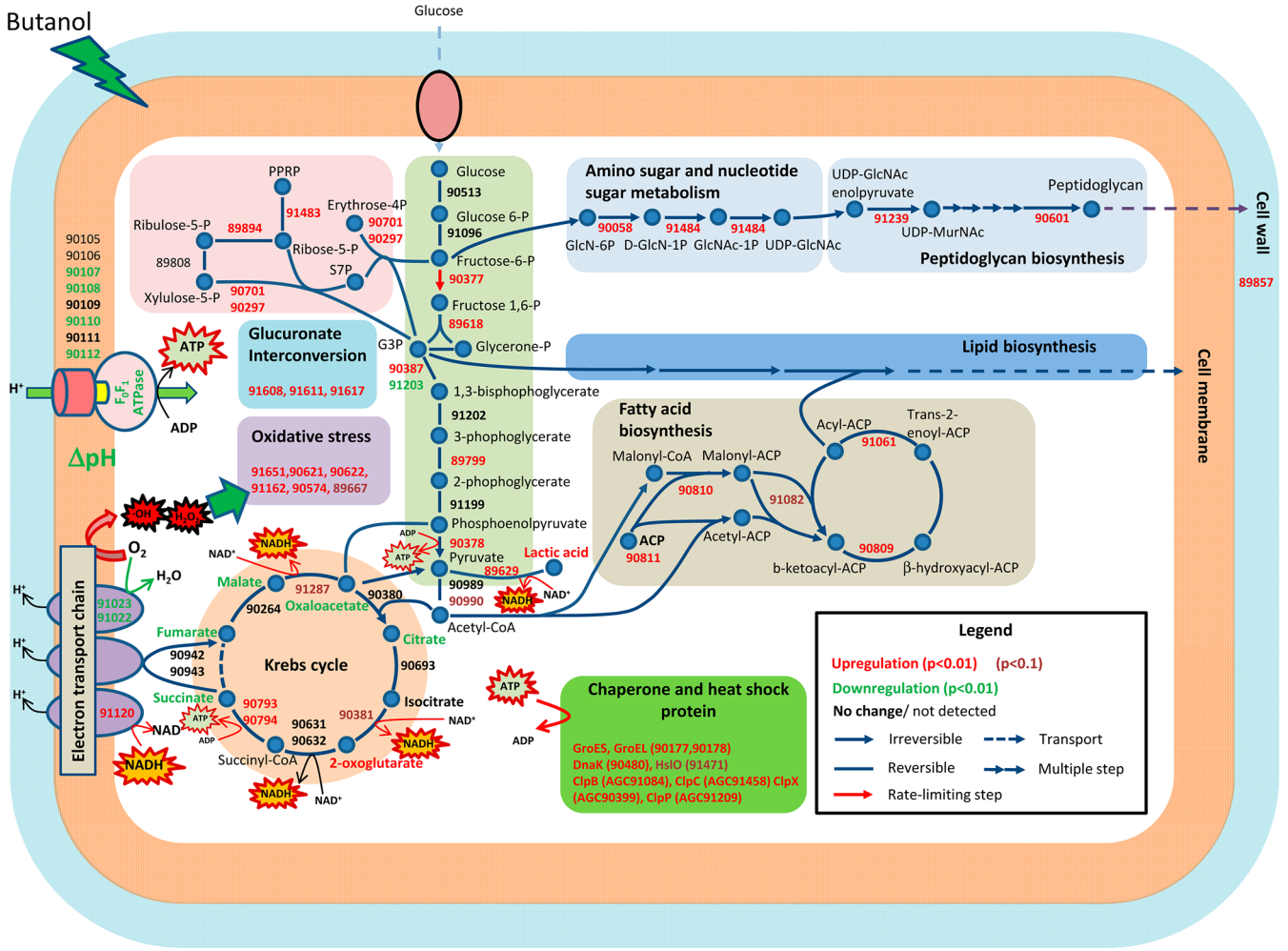

Figure 3. Overall schematic representation of the dynamic responses in *S. warneri* SG1 upon exposure to 1.5% butanol. Accession numbers for proteins which were up-regulated at least 1.5-fold (p-value < 0.01) are marked in red, whereas those corresponding to proteins which were down-regulated by at least 0.67-fold are marked in green. Metabolites are represented by circles while ATP and NADH are also highlighted.

to strengthen it.[49,50] Altogether, the increased expression of cell wall synthesis/modification enzymes suggests an elaborate adaptive mechanism for SG1 to survive in the presence of butanol.

Changes in fatty acid and phospholipid compositions upon solvent exposure are well documented for both Gram-negative and Gram-positive bacteria. However, the reported effects were contradictory. Studies done on *E. coli* and *P. putida* demonstrated denser membrane packing and therefore a decrease in membrane fluidity upon organic solvent exposure.[6] In contrast, *Staphylococcus hemolyticus* and *Bacillus* sp. strain ORAs2 adapted to solvent challenge by increasing membrane fluidity.[7,51] In this study, we found a branched-chain amino acid transaminase (AGC91419) was up-regulated 1.5-fold. This protein initiates the first step of branched fatty acids synthesis by converting isoleucine, leucine, and valine to the corresponding α-keto acids. Thus, it appears that SG1 is increasing the membrane fluidity in order to combat butanol stress. Several other enzymes involved in the fatty acid synthesis machinery were also up-regulated in the presence of butanol. Malonyl CoA-acyl carrier protein transacylase (AGC90810), 3-oxoacyl-[acyl-carrier protein] reductase (AGC90809), and enoyl-[acyl-carrier protein] reductase I (FAGC91061) were all up-regulated (Figure 3), indicating enhanced production of fatty acids in SG1 under butanol stress. Finally, we observed a 2.1-fold up-regulation of the fatty acid/phospholipid synthesis protein PlsX (AGC90811), which has been shown to catalyze the synthesis of fatty acyl-phosphate[52] and postulated to play a role in fatty acid metabolism by regulating the intracellular concentration of acyl-[acyl carrier protein].[53] The *plsX* gene is part of a locus that comprises genes encoding 3-oxoacyl-[acyl-carrier protein] reductase and enoyl-[acyl-carrier protein] reductase mentioned above, as well as a gene encoding for a fatty acid biosynthesis transcriptional regulator (AGC90812). Altogether, it appears that up-regulation of fatty acid synthesis enzymes under the $BtOH^+$ condition allows SG1 to overcome butanol stress by increasing fatty acid synthesis, especially those which contain branched chains to increase the overall membrane fluidity.

Changes in Energy Metabolism

A key mechanism of solvent toxicity is the partition of the solvent into the cytoplasmic membrane, causing leakage of ions and small molecules across the lipid bilayer.[54−56] The loss of the proton gradient and membrane potential leads to deprivation in ATP synthesis and inhibition of transport processes that are coupled to the proton motive force. In SG1, the enzymes involved in oxidative phosphorylation are differentially regulated upon butanol challenge: the soluble

dx.doi.org/10.1021/pr400533m | J. Proteome Res. 2013, 12, 4478−4489

NADH dehydrogenase (AGC91120) was up-regulated >5-fold; expression of the succinate dehydrogenase complex was unchanged; the terminal cytochrome *aa*3 oxidase (AGC91022, subunit II; AGC91023, subunit I) and ATP synthase (AGC90107, B subunit of F_0; AGC90108, δ subunit of F_1; AGC90110, γ subunit of F_1; AGC90112, ε subunit of F_1) were down-regulated ∼2-fold (Figure 3). Different studies in the literature show that ATP synthase can be either down-regulated[21,57] or up-regulated[23,45] upon solvent stress.

To compensate for the decreased level of energy production from oxidative phosphorylation, cells must utilize other methods of ATP generation, such as substrate level phosphorylation. In our 2-MEGA labeling study on SG1, the majority of proteins that are involved in glycolysis and the tricarboxylic acid cycle were either unchanged or up-regulated upon butanol challenge (Figure 2B, COG class G). Interestingly, we observed the key reactions of these pathways to be highly influenced by the presence of butanol (Figure 3). In glycolysis, the irreversible conversion of β-D-fructose 6-phosphate to β-D-fructose 1,6-bisphosphate represents a crucial rate-limiting step. Phosphofructokinase (AGC90377), the enzyme that catalyzes this reaction, was up-regulated 3.4-fold when cells were grown in the presence of butanol. The final enzyme in glycolysis, pyruvate kinase (AGC90378), generates ATP at the substrate level and was up-regulated 1.9-fold under the $BtOH^+$ condition. In the tricarboxylic acid cycle, succinyl-CoA synthetase (α subunit, AGC90793; β subunit, AGC90794) can also generate either ATP or GTP, and it was up-regulated 3.8-fold. Enzymes that are involved in NADH generation, such as glyceraldehyde 3-phosphate dehydrogenase (AGC90387) and malate dehydrogenase (AGC90287), were also up-regulated (Figure 3). The increased expression of key proteins involved in the central carbohydrate metabolic pathways is undoubtedly a cellular response to compensate for the decreased ATP synthesis from oxidative phosphorylation and to meet the high energy demands of combating butanol stress.[23,45,57]

Comparative genomics between *S. warneri* SG1 and other *Staphylococci* species suggested a number of gene products which may contribute to the solvent tolerance properties of SG1.[11] One distinction is the presence of a gene cluster that encodes for enzymes involved in glucuronate interconversion (AGC91608−AGC91617). The proteins D-mannonate oxidoreductase (AGC91609), 2-keto-3-deoxygluconate kinase (AGC91613), and 4-hydroxy-2-oxoglutarate aldolase (AGC91614) were observed only in the $BtOH^+$ condition. 2-MEGA labeling showed that β-D-glucuronidase (AGC91608), glucuronate isomerase (AGC91611), and β-*N*-acetylhexosaminidase (AGC91617) were induced 14.0-fold, 2.8-fold, 2.1-fold, respectively. Thus, the majority of the enzymes in this locus involved in glucuronate interconversion appear to be highly upregulated upon butanol exposure. To our knowledge, this is the first report of a positive correlation between glucuronate interconversion and solvent tolerance and their mechanistic relationship is unclear. One possibility is that these unusual sugars are used to synthesize a hydrophilic extracellular capsule to repel organic solvents,[58] as exemplified by *S. warneri* ZZ1 upon toluene exposure.[8,58]

Global Stress Responses

Exposure to organic solvents typically triggers a global cellular response involving heat shock proteins, oxidative stress proteins, and transcriptional activators/repressors.[6,58,59] The 2-MEGA labeling studies showed that butanol exposure to SG1 resulted in COG class O (post-translational modification, protein turnover, chaperones) being the second most elevated COG class only behind carbohydrate transport and metabolism (Figure 2B). Interestingly, the most up-regulated proteins in COG class O upon butanol challenge were a hypothetical protein with a NifU-like domain (AGC91125) and an iron−sulfur cluster assembly protein SufC (AGC91149), which were increased 17.2 and 4.7-fold, respectively. In plants and bacteria, the NifU protein acts as a scaffold for iron−sulfur cluster formation.[60,61] The up-regulation of a NifU-like protein along with SufC suggests that iron−sulfur cluster proteins in SG1 were damaged in the presence of butanol. If this is true, then labile iron from damaged proteins could lead to increased oxidative stress in the cell and trigger repair proteins to counteract oxidative damage.

A number of proteins belonging to the Clp superfamily of proteases were induced at least 1.5-fold in the $BtOH^+$ condition (Figure 3, Supporting Information Table S4: ClpC, AGC91458; ClpX, AGC90399; ClpB, AGC91084; ClpP, AGC91209). In *S. aureus*, the proteolytic activity of ClpP is critical for pathogenicity, stress response, metal homeostasis, prevention of autolysis, and activation of the heat shock regulon.[62,63] The Clp proteases are also activated upon solvent stress in the strict anaerobe *C. acetobutylicum*.[19,20,64] In agreement with those studies, several other molecular chaperones, notably DnaK (AGC90480), GroES (AGC90177), and GroEL (AGC90178), were also induced in SG1 in the presence of butanol.

In addition to the chaperones and Clp proteases, we also observed increased abundances of two Zn-containing alcohol dehydrogenases (AGC90034 and AGC91651) and an aldehyde dehydrogenase (AGC90092) that could potentially help combat oxidative stress. Interestingly, we also saw up-regulation of methionine-(*S*)-sulfoxide reductase (MsrA, AGC90621) and methionine-(*R*)-sulfoxide reductase (MsrB, AGC90622) by 1.6-fold and 1.9-fold, respectively, in the $BtOH^+$ condition. As shown in studies on other bacterial models, MsrA, as well as MsrB to a lesser extent, are crucial for the amelioration of cellular damage from reactive oxygen species.[65,66] Finally, peroxiredoxin (OsmC, AGC91162) was also up-regulated 2.5-fold in SG1 upon butanol challenge. This ubiquitous redox sensitive protein is a good biomarker for oxidative stress.[67,68] The combination of proteases, molecular chaperones, redox sensors, and scavengers of reactive oxygen species which are up-regulated paints a strong picture of oxidative stress induction in SG1 in the presence of butanol.

Metabolomic Study

In our metabolomics study, we applied a differential isotopic labeling technique to target the amine-, phenol- and acid-containing submetabolomes. The comparison between abundances of $BtOH^-$ and $BtOH^+$ metabolites was based on the ratio of ^{12}C-labeled individual samples to the ^{13}C-labeled pooled reference sample.[24,25] This labeling technique allows sensitivity enhancement of 10- to 1000-fold and is particularly useful for monitoring amino acids, polyamines, and organic acids in biological samples. Although global metabolite profiling using techniques, such as NMR and LC−MS without isotope labeling, was not performed in this study, the profiling of targeted submetabolomes with enhanced metabolite detection is informative. Using this approach, a large fraction of the metabolites associated with a particular metabolic network of

interest, such as the TCA cycle, can be profiled, which provides more accurate information on cellular metabolic processes. As we will see below, these compounds play an important role in response to butanol stress and a correlation with the proteomics results can be observed.

Analysis of Amine- and Phenol-Containing Metabolites

On average, 605 ± 86 peak pairs or putative metabolites were extracted from duplicate experiments on triplicate $BtOH^-$ and $BtOH^+$ samples. Principal component analysis was first applied to evaluate whether the addition of butanol had an effect on the metabolite profiles of SG1. As shown in Figure 4, there was a clear distinction between $BtOH^-$ and $BtOH^+$ cultures, and the separation is mainly reflected by the first principal component, indicating that the presence of butanol lead to a significant alteration of the metabolite levels in SG1. Using a volcano plot to find individual metabolites which varied by at least 1.5-fold with a *p*-value smaller than 0.01, we identified 94 metabolites, among which 15 were unambiguously identified (see Table 1).

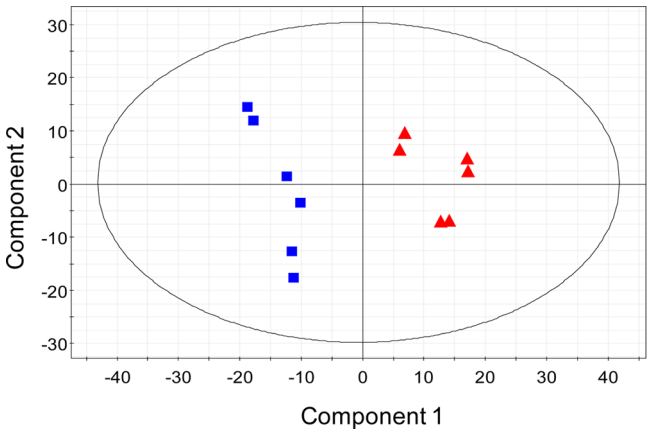

Figure 4. Principal component analysis plot of dansylation labeled metabolites from *S. warneri* SG1 grown in $BtOH^-$ or $BtOH^+$ medium. The data was from technical duplicate experiments on biological triplicate samples of $BtOH^-$ and $BtOH^+$ lysates. Red triangles and blue squares represent $BtOH^-$ and $BtOH^+$ cultures, respectively.

As discussed above, butanol stress is linked to the oxidative stress response. We detected higher cadaverine/lysine (Figure 5A) and putrescine/ornithine ratios (Figure 5B), which is consistent with the up-regulation of Orn/Lys/Arg decarboxylase (AGC91502) in our proteomics data. Cadaverine is a scavenger of superoxide radicals during oxidative stress.[69] Spermine, a polyamine which can protect DNA from free radical attack[70] and inhibit autolysis of Gram-negative marine pseudomonad NCMB 845,[71,72] was also up-regulated in $BtOH^+$ SG1. Interestingly, *S. warneri* SG1 is not predicted to encode a spermine synthase protein, and the physiological function of spermine in bacteria has not been elucidated.[73] A negative aspect of spermine accumulation is the cytotoxicity and inhibition of cell growth.[74] However, the enzyme spermine/spermidine acetyl-transferase can minimize the cytotoxicity of spermine by converting it into *N*1-acetyl-spermine,[74] and a similar enzyme (AGC91503) is present in the SG1 genome. Although we only detected the presence of AGC91503 in proteome profiling and failed to quantify it in the 2MEGA labeling, the amount of *N*1-acetyl-spermine observed was increased considerably in $BtOH^+$ sample (Figure 5C), which suggests the enhanced activity of AGC91503 in the presence of butanol.

The conversion of methionine to methionine sulfoxide is another commonly observed reaction under oxidative stress conditions, wherein methionine can react with reactive oxygen species via a two-electron-dependent mechanism to produce methionine sulfoxide.[75] Our metabolomics data show that the ratio of methionine sulfoxide/methionine in $BtOH^+$ increased more than 2.5-fold compared to that in $BtOH^-$ (Figure 5D), indicating an increased level of oxidation in response to the oxidative stress caused by butanol. The up-regulation of MsrA and MsrB (discussed above) would allow rapid regeneration of methionine from methionine sulfoxide, allowing continuous disposition of reactive oxygen species.

Analysis of TCA Cycle Carboxylic Acids

Prior to isotopic labeling, an extraction step was carried out to remove amine-containing compounds in order to increase the specificity of the reaction for carboxylic acids. With the optimized sample loading, an average of 449 ± 66 peak pairs or putative metabolites were extracted from duplicate experiments on triplicate $BtOH^-$ and $BtOH^+$ samples. In this study, we focused on obtaining dynamic changes of seven TCA cycle carboxylic acids in the presence of butanol (Supporting Information Table S5), as the TCA cycle is a critical energy metabolic pathway and the changes in metabolite levels in TCA

Table 1. List of Differentially Expressed Amine-Containing Metabolites That Were Unambiguously Identified[a]

metabolite name	fold change	*p*-value	avg rt (min)	*m/z* (light)	*m/z* (heavy)
N1-acetylspermine	21.64	7.17×10^{-8}	25.1	315.4672	317.4742
spermine	6.76	1.65×10^{-5}	28.9	379.1478	381.8232
cadaverine	3.99	3.83×10^{-3}	23.6	285.1158	287.1226
arginine	2.21	1.46×10^{-4}	4.4	408.1703	410.1769
pyrrolidinone	1.97	2.80×10^{-4}	15.7	319.1115	321.1181
γ-aminobutyric acid	1.89	6.16×10^{-4}	9.9	337.1220	339.1287
threonine	1.70	1.32×10^{-3}	8.0	353.1172	355.1239
taurine	0.61	2.71×10^{-3}	3.9	359.0734	361.0800
methionine sulfoxide	0.53	6.98×10^{-3}	6.8	399.1046	401.1115
glucosamine	0.47	7.94×10^{-5}	4.4	413.1383	415.1450
lysine	0.35	6.43×10^{-4}	19.8	307.1115	309.1183
spermidine	0.30	1.65×10^{-6}	26.1	423.1640	426.1741
ornithine	0.30	3.08×10^{-4}	18.7	300.1014	302.1082
methionine	0.21	9.02×10^{-4}	13.3	383.1099	385.1166

[a]The fold change represents the levels of metabolite seen in $BtOH^+$ versus $BtOH^-$.

dx.doi.org/10.1021/pr400533m | J. Proteome Res. 2013, 12, 4478−4489

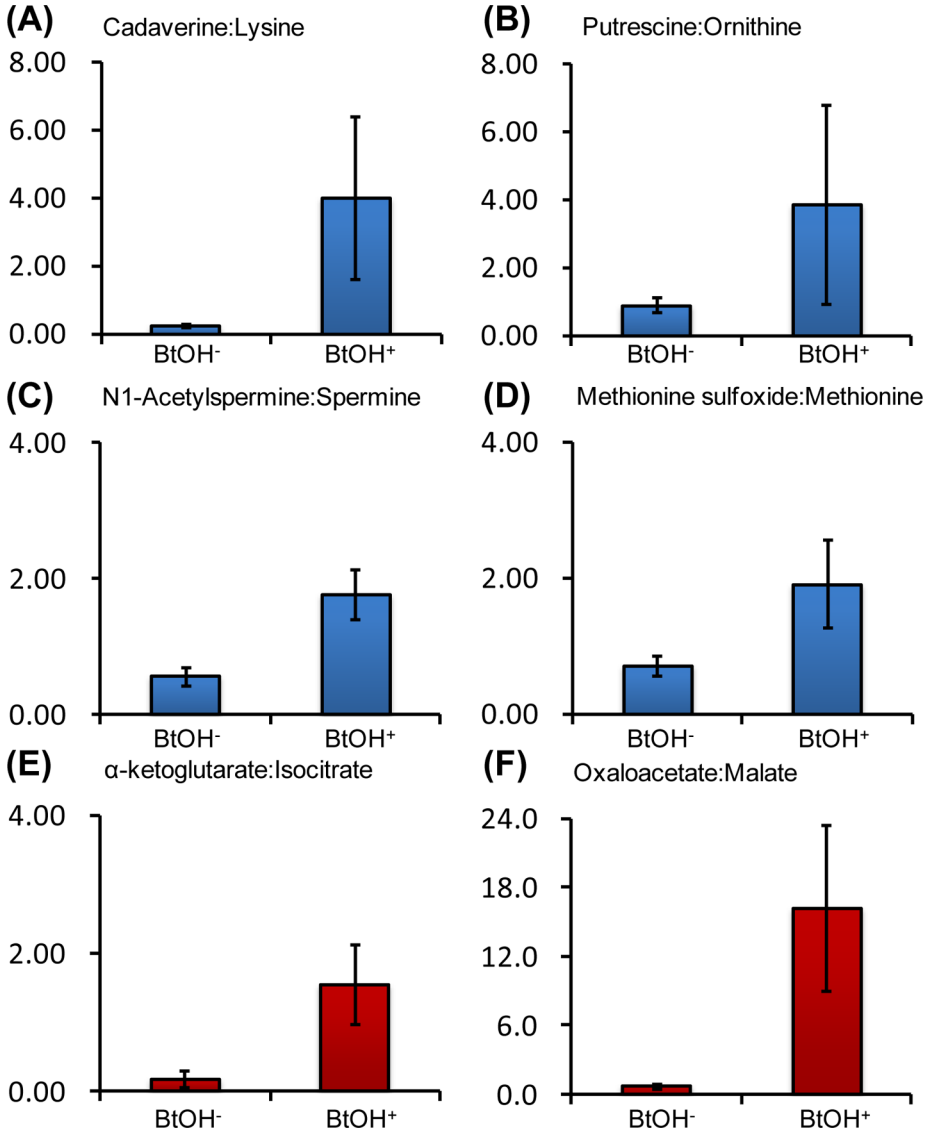

Figure 5. Column plots highlighting product:substrate ratios which were increased upon butanol challenge. The data was from technical duplicate experiments on triplicate $BtOH^-$ and $BtOH^+$ cultures.

cycle reflects the regulation of energy metabolism of SG1 under butanol stress.

From the 2D-LC–MS/MS proteomic studies, we observed up-regulation of enzymes responsible for critical energy-producing reactions in the TCA cycle. In agreement, the acid profiling results show that the α-ketoglutarate:isocitrate (Figure 5E) and oxaloacetate/malate ratios (Figure 5F) were increased significantly under butanol challenge. The isocitrate dehydrogenase (isocitrate → α-ketoglutarate) and malate dehydrogenase (malate → oxaloacetate) reactions both produce NADH, which is fed into the oxidative phosphorylation pathway to produce ATP. Interestingly, the other reaction that generates NADH in the TCA cycle, the α-ketoglutarate dehydrogenase reaction (α-ketoglutarate → succinyl-CoA), was not up-regulated as indicated by the high level of α-ketoglutarate in $BtOH^+$ cells. This could be explained by considering that the enzyme is sensitive to oxidative stress and can be inhibited under such conditions.[76] Since α-ketoglutarate itself can act as an effective scavenger of reactive oxygen species, the stress condition should favor an increased accumulation of α-ketoglutarate.[77] Looking at the downstream intermediates, we saw decreased levels of succinate, fumarate, and malate. Our results indicate that the TCA cycle plays a key role in regulation of the cell response to butanol stress, as it not only promotes the production of energy, but also helps to modulate the oxidative stress condition induced by butanol.

■ CONCLUSIONS

Understanding the complex interplay that results in solvent tolerance can shed light on how to genetically engineer bacteria for biodegradation, biofuel production, and biocatalysis. Our comprehensive proteomic and metabolomic study on SG1 reveals a complicated mechanism for butanol adaptation that spans multiple clusters of orthologous groups. Upon butanol challenge, the structure and composition of cell wall/membrane were altered. We also saw a strong link between solvent stress and oxidative stress. Many stress response proteins such as chaperones and proteases were up-regulated upon butanol challenge. Key enzymes in carbohydrate metabolism, including those involved in glucuronate interconversions, were also up-regulated to counteract the drop in ATP synthesis via oxidative phosphorylation. Consistent with the proteomic study, inter-

dx.doi.org/10.1021/pr400533m | J. Proteome Res. 2013, 12, 4478–4489

rogation of amine- and phenol- containing metabolites provided strong evidence of oxidative stress when SG1 was exposed to butanol. Analysis of TCA cycle metabolites further confirmed these observations and also indicated the key role of TCA cycle intermediates in the mechanism of butanol tolerance of SG1.

The vast proteomic changes observed in SG1 upon butanol challenge observed in our study suggests that a reductionist approach (a single gene leading to a specific phenotype) to study solvent tolerance is far from ideal. However, it would still be of great interest to determine whether overexpression of specific proteins, such as those involved in oxidative stress or at key metabolic junctures, can lead to solvent tolerance. In addition to genetic engineering, modification of the growth conditions (different carbon/nitrogen sources, aerobic versus anaerobic growth, etc.) might allow growth in a higher titer of organic solvent by minimizing energy consumption and reducing the basal level of oxidative stress. Perhaps this explains why *C. acetobutylicum*, a strict anaerobe, is highly tolerant to butanol and ethanol. Altogether, the results presented in this work greatly enrich our knowledge of the mechanisms employed by SG1 to combat butanol toxicity.

■ ASSOCIATED CONTENT

Supporting Information

Experimental workflow of 2-MEGA isotopic labeling (Figure S1); $\log_2$–$\log_2$ plots of peptide ratios from the forward ($BtOH^+_L$:$BtOH^-_H$) and reverse ($BtOH^+_H$:$BtOH^-_L$) labeling (Figure S2); summary of *S. warneri* SG1 grown in the presence of organic solvents (Supplemental Table S1); summary of protein identification of *S. warneri* SG1 cultured in $BtOH^+$ or $BtOH^-$ medium (Table S2); list of the most abundant proteins in the *S. warneri* SG1 $BtOH^-$ and $BtOH^+$ proteomes (Table S3); list of differentially expressed proteins from *S. warneri* SG1 cultured in $BtOH^+$ or $BtOH^-$ medium (Table S4); levels of carboxylic acid-containing metabolites in the TCA cycle (Table S5). This material is available free of charge via the Internet at http://pubs.acs.org.

■ AUTHOR INFORMATION

Corresponding Authors

*E-mail: Liang.Li@ualberta.ca. Tel: 780-492-3250. Fax: 780-492-8231.
*E-mail: Joel.Weiner@ualberta.ca. Tel: 780-492-2761. Fax: 780-492-2558.

Notes

The authors declare no competing financial interest.

■ ACKNOWLEDGMENTS

This work was funded by the Natural Sciences and Engineering Research Council of Canada, the Canada Research Chair program, Genome Canada and Genome Alberta, and the Biorefining Conversions Network of Alberta Innovates Biosolutions.

■ REFERENCES

(1) Sikkema, J.; de Bont, J. A.; Poolman, B. Mechanisms of membrane toxicity of hydrocarbons. *Microbiol. Rev.* **1995**, *59* (2), 201–22.
(2) Isken, S.; de Bont, J. A. M. Bacteria tolerant to organic solvents. *Extremophiles* **1998**, *2* (3), 229–238.
(3) Sardessai, Y.; Bhosle, S. Tolerance of bacteria to organic solvents. *Res. Microbiol.* **2002**, *153* (5), 263–268.
(4) Ramos, J. L.; Duque, E.; Gallegos, M. T.; Godoy, P.; Ramos-Gonzalez, M. I.; Rojas, A.; Teran, W.; Segura, A. Mechanisms of solvent tolerance in Gram-negative bacteria. *Ann. Rev. Microbiol.* **2002**, *56*, 743–768.
(5) Nicolaou, S. A.; Gaida, S. M.; Papoutsakis, E. T. A comparative view of metabolite and substrate stress and tolerance in microbial bioprocessing: From biofuels and chemicals, to biocatalysis and bioremediation. *Metab. Eng.* **2010**, *12* (4), 307–331.
(6) Segura, A.; Molina, L.; Fillet, S.; Krell, T.; Bernal, P.; Munoz-Rojas, J.; Ramos, J. L. Solvent tolerance in Gram-negative bacteria. *Curr. Opin. Biotechnol.* **2012**, *23* (3), 415–421.
(7) Nielsen, L. E.; Kadavy, D. R.; Rajagopal, S.; Drijber, R.; Nickerson, K. W. Survey of extreme solvent tolerance in Gram-positive cocci: membrane fatty acid changes in Staphylococcus haemolyticus grown in toluene. *Appl. Environ. Microbiol.* **2005**, *71* (9), 5171–5176.
(8) Zahir, Z.; Seed, K. D.; Dennis, J. J. Isolation and characterization of novel organic solvent-tolerant bacteria. *Extremophiles* **2006**, *10* (2), 129–138.
(9) Grandvalet, C.; Assad-Garcia, J. S.; Chu-Ky, S.; Tollot, M.; Guzzo, J.; Gresti, J.; Tourdot-Marechal, R. Changes in membrane lipid composition in ethanol- and acid-adapted *Oenococcus oeni* cells: characterization of the cfa gene by heterologous complementation. *Microbiology* **2008**, *154* (Pt 9), 2611–2619.
(10) Gao, Y.; Dai, J.; Peng, H.; Liu, Y.; Xu, T. Isolation and characterization of a novel organic solvent-tolerant *Anoxybacillus* sp. PGDY12, a thermophilic Gram-positive bacterium. *J. Appl. Microbiol.* **2011**, *110* (2), 472–478.
(11) Cheng, V. W.; Zhang, G.; Oyedotun, K. S.; Ridgway, D.; Ellison, M. J.; Weiner, J. H. Complete Genome of the Solvent-Tolerant *Staphylococcus warneri* Strain SG1. *Genome Announce.* **2013**, *1* (2), e0003813.
(12) Jones, D.; Woods, D. Acetone-butanol fermentation revisited. *Microbiol. Rev.* **1986**, *50*, 484–524.
(13) Bermejo, L. L.; Welker, N. E.; Papoutsakis, E. T. Expression of *Clostridium acetobutylicum* ATCC 824 genes in *Escherichia coli* for acetone production and acetate detoxification. *Appl. Environ. Microbiol.* **1998**, *64* (3), 1079–1085.
(14) Steen, E.; Chan, R.; Prasad, N.; Myers, S.; Petzold, C.; Redding, A.; Ouellet, M.; Keasling, J. Metabolic engineering of *Saccharomyces cerevisiae* for the production of n-butanol. *Microb. Cell Fact.* **2008**, 7–36.
(15) Atsumi, S.; Cann, A.; Connor, M.; Shen, C.; Smith, K.; Brynildsen, M.; Chou, K.; Hanai, T.; Liao, J. Metabolic engineering of *Escherichia coli* for 1-butanol production. *Metab. Eng.* **2008**, *10*, 305–311.
(16) Atsumi, S.; Hanai, T.; Liao, J. C. Non-fermentative pathways for synthesis of branched-chain higher alcohols as biofuels. *Nature* **2008**, *451* (7174), 86–89.
(17) Tomas, C. A.; Beamish, J.; Papoutsakis, E. T. Transcriptional analysis of butanol stress and tolerance in *Clostridium acetobutylicum*. *J. Bacteriol.* **2004**, *186* (7), 2006–2018.
(18) Brynildsen, M. P.; Liao, J. C. An integrated network approach identifies the isobutanol response network of *Escherichia coli*. *Mol. Syst. Biol.* **2009**, *5*, 277.
(19) Alsaker, K. V.; Paredes, C.; Papoutsakis, E. T. Metabolite stress and tolerance in the production of biofuels and chemicals: gene-expression-based systems analysis of butanol, butyrate, and acetate stresses in the anaerobe *Clostridium acetobutylicum*. *Biotechnol. Bioeng.* **2010**, *105* (6), 1131–1147.
(20) Mao, S.; Luo, Y.; Zhang, T.; Li, J.; Bao, G.; Zhu, Y.; Chen, Z.; Zhang, Y.; Li, Y.; Ma, Y. Proteome Reference Map and Comparative Proteomic Analysis between a Wild Type *Clostridium acetobutylicum* DSM 1731 and its Mutant with Enhanced Butanol Tolerance and Butanol Yield. *J. Proteome Res.* **2010**, *9* (6), 3046–3061.
(21) Mao, S.; Luo, Y.; Bao, G.; Zhang, Y.; Li, Y.; Ma, Y. Comparative analysis on the membrane proteome of *Clostridium acetobutylicum* wild

type strain and its butanol-tolerant mutant. *Mol. BioSyst.* **2011**, *7* (5), 1660−1677.
(22) Segura, A.; Godoy, P.; van Dillewijn, P.; Hurtado, A.; Arroyo, N.; Santacruz, S.; Ramos, J. L. Proteomic analysis reveals the participation of energy- and stress-related proteins in the response of *Pseudomonas putida* DOT-T1E to toluene. *J. Bacteriol.* **2005**, *187* (17), 5937−5945.
(23) Wijte, D.; van Baar, B. L.; Heck, A. J.; Altelaar, A. F. Probing the proteome response to toluene exposure in the solvent tolerant Pseudomonas putida S12. *J. Proteome Res.* **2011**, *10* (2), 394−403.
(24) Guo, K.; Li, L. Differential 12C-/13C-Isotope Dansylation Labeling and Fast Liquid Chromatography/Mass Spectrometry for Absolute and Relative Quantification of the Metabolome. *Anal. Chem.* **2009**, *81* (10), 3919−3932.
(25) Guo, K.; Li, L. High-Performance Isotope Labeling for Profiling Carboxylic Acid-Containing Metabolites in Biofluids by Mass Spectrometry. *Anal. Chem.* **2010**, *82* (21), 8789−8793.
(26) Ye, X.; Li, L. Microwave-Assisted Protein Solubilization for Mass Spectrometry-Based Shotgun Proteome Analysis. *Anal. Chem.* **2012**, *84* (14), 6181−6191.
(27) Wang, N.; Xie, C.; Young, J. B.; Li, L. Off-Line Two-Dimensional Liquid Chromatography with Maximized Sample Loading to Reversed-Phase Liquid Chromatography-Electrospray Ionization Tandem Mass Spectrometry for Shotgun Proteome Analysis. *Anal. Chem.* **2009**, *81* (3), 1049−1060.
(28) Wang, N.; Li, L. Exploring the Precursor Ion Exclusion Feature of Liquid Chromatography−Electrospray Ionization Quadrupole Time-of-Flight Mass Spectrometry for Improving Protein Identification in Shotgun Proteome Analysis. *Anal. Chem.* **2008**, *80* (12), 4696−4710.
(29) Elias, J. E.; Gygi, S. P. Target-decoy search strategy for increased confidence in large-scale protein identifications by mass spectrometry. *Nat. Methods* **2007**, *4* (3), 207−214.
(30) Ishihama, Y.; Oda, Y.; Tabata, T.; Sato, T.; Nagasu, T.; Rappsilber, J.; Mann, M. Exponentially modified protein abundance index (emPAI) for estimation of absolute protein amount in proteomics by the number of sequenced peptides per protein. *Mol. Cell. Proteomics* **2005**, *4* (9), 1265−1272.
(31) Ji, C.; Guo, N.; Li, L. Differential dimethyl labeling of N-termini of peptides after guanidination for proteome analysis. *J. Proteome Res.* **2005**, *4* (9), 2099−2108.
(32) Lo, A.; Tang, Y.; Chen, L.; Li, L. Automation of dimethylation after guanidination labeling chemistry and its compatibility with common buffers and surfactants for mass spectrometry-based shotgun quantitative proteome analysis. *Anal. Chim. Acta* **2013**, *788* (0), 81−88.
(33) Wang, P.; Lo, A.; Young, J. B.; Song, J. H.; Lai, R.; Kneteman, N. M.; Hao, C. H.; Li, L. Targeted Quantitative Mass Spectrometric Identification of Differentially Expressed Proteins between Bax-Expressing and Deficient Colorectal Carcinoma Cells. *J. Proteome Res.* **2009**, *8* (7), 3403−3414.
(34) Tian, X.; Chen, L.; Wang, J.; Qiao, J.; Zhang, W. Quantitative proteomics reveals dynamic responses of *Synechocystis* sp. PCC 6803 to next-generation biofuel butanol. *J. Proteomics* **2013**, *78*, 326−345.
(35) Hilger, M.; Mann, M. Triple SILAC to determine stimulus specific interactions in the Wnt pathway. *J. Proteome Res.* **2012**, *11* (2), 982−994.
(36) Tatusov, R. L.; Galperin, M. Y.; Natale, D. A.; Koonin, E. V. The COG database: a tool for genome-scale analysis of protein functions and evolution. *Nucleic Acids Res.* **2000**, *28* (1), 33−36.
(37) Ogata, H.; Goto, S.; Sato, K.; Fujibuchi, W.; Bono, H.; Kanehisa, M. KEGG: Kyoto Encyclopedia of Genes and Genomes. *Nucleic Acids Res.* **1999**, *27* (1), 29−34.
(38) Wu, Y. M.; Li, L. Determination of Total Concentration of Chemically Labeled Metabolites as a Means of Metabolome Sample Normalization and Sample Loading Optimization in Mass Spectrometry-Based Metabolomics. *Anal. Chem.* **2012**, *84* (24), 10723−10731.
(39) Smith, C. A.; Want, E. J.; O'Maille, G.; Abagyan, R.; Siuzdak, G. XCMS: Processing Mass Spectrometry Data for Metabolite Profiling Using Nonlinear Peak Alignment, Matching, and Identification. *Anal. Chem.* **2006**, *78* (3), 779−787.
(40) Guo, K.; Peng, J.; Zhou, R.; Li, L. Ion-pairing reversed-phase liquid chromatography fractionation in combination with isotope labeling reversed-phase liquid chromatography−mass spectrometry for comprehensive metabolome profiling. *J. Chromatogr., A* **2011**, *1218* (23), 3689−3694.
(41) Sivagnanam, K.; Raghavan, V.; Shah, M.; Hettich, R.; Verberkmoes, N.; Lefsrud, M. Comparative shotgun proteomic analysis of *Clostridium acetobutylicum* from butanol fermentation using glucose and xylose. *Proteome Sci.* **2011**, *9* (1), 66.
(42) Becher, D.; Hempel, K.; Sievers, S.; Zuhlke, D.; Pane-Farre, J.; Otto, A.; Fuchs, S.; Albrecht, D.; Bernhardt, J.; Engelmann, S.; Volker, U.; van Dijl, J. M.; Hecker, M. A proteomic view of an important human pathogen–towards the quantification of the entire *Staphylococcus aureus* proteome. *PLoS One* **2009**, *4* (12), e8176.
(43) Hempel, K.; Herbst, F.-A.; Moche, M.; Hecker, M.; Becher, D. Quantitative proteomic view on secreted, cell surface-associated, and cytoplasmic proteins of the methicillin-resistant human pathogen *Staphylococcus aureus* under iron-limited conditions. *J. Proteome Res.* **2011**, *10* (4), 1657−1666.
(44) Tatusov, R. L.; Galperin, M. Y.; Natale, D. A.; Koonin, E. V. The COG database: a tool for genome-scale analysis of protein functions and evolution. *Nucleic Acids Res.* **2000**, *28* (1), 33−36.
(45) Rutherford, B. J.; Dahl, R. H.; Price, R. E.; Szmidt, H. L.; Benke, P. I.; Mukhopadhyay, A.; Keasling, J. D. Functional genomic study of exogenous n-butanol stress in Escherichia coli. *Appl. Environ. Microbiol.* **2010**, *76* (6), 1935−1945.
(46) Schindler, C. A.; Schuhardt, V. T. Lysostaphin: A New Bacteriolytic Agent for the Staphylococcus. *Proc. Natl. Acad. Sci. U.S.A.* **1964**, *51*, 414−21.
(47) Browder, H. P.; Zygmunt, W. A.; Young, J. R.; Tavormina, P. A. Lysostaphin: Enzymatic Mode of Action. *Biochem. Biophys. Res. Commun.* **1965**, *19*, 383−389.
(48) Silhavy, T. J.; Kahne, D.; Walker, S. The bacterial cell envelope. *Cold Spring Harbor Perspect. Biol.* **2010**, *2* (5), a000414.
(49) Reith, J.; Mayer, C. Peptidoglycan turnover and recycling in Gram-positive bacteria. *Appl. Microbiol. Biotechnol.* **2011**, *92* (1), 1−11.
(50) Weidenmaier, C.; Peschel, A. Teichoic acids and related cell-wall glycopolymers in Gram-positive physiology and host interactions. *Nat. Rev. Microbiol.* **2008**, *6* (4), 276−287.
(51) Pepi, M.; Heipieper, H. J.; Fischer, J.; Ruta, M.; Volterrani, M.; Focardi, S. E. Membrane fatty acids adaptive profile in the simultaneous presence of arsenic and toluene in *Bacillus* sp. ORAs2 and *Pseudomonas* sp. ORAs5 strains. *Extremophiles* **2008**, *12* (3), 343−349.
(52) Lu, Y. J.; Zhang, Y. M.; Grimes, K. D.; Qi, J.; Lee, R. E.; Rock, C. O. Acyl-phosphates initiate membrane phospholipid synthesis in Gram-positive pathogens. *Mol. Cell* **2006**, *23* (5), 765−772.
(53) Yoshimura, M.; Oshima, T.; Ogasawara, N. Involvement of the YneS/YgiH and PlsX proteins in phospholipid biosynthesis in both Bacillus subtilis and Escherichia coli. *BMC Microbiol.* **2007**, *7* (1), 69.
(54) Cartwright, C. P.; Juroszek, J.-R.; Beavan, M. J.; Ruby, F. M. S.; De Morais, S. M. F.; Rose, A. H. Ethanol Dissipates the Proton-motive Force across the Plasma Membrane of *Saccharomyces cerevisiae*. *J. Gen. Microbiol.* **1986**, *132* (2), 369−377.
(55) Leao, C.; Van Uden, N. Effects of ethanol and other alkanols on passive proton influx in the yeast *Saccharomyces cerevisiae*. *Biochim. Biophys. Acta* **1984**, *774* (1), 43−48.
(56) Bowles, L. K.; Ellefson, W. L. Effects of butanol on *Clostridium acetobutylicum*. *Appl. Environ. Microbiol.* **1985**, *50* (5), 1165−1170.
(57) Volkers, R. J.; de Jong, A. L.; Hulst, A. G.; van Baar, B. L.; de Bont, J. A.; Wery, J. Chemostat-based proteomic analysis of toluene-affected *Pseudomonas putida* S12. *Environ. Microbiol.* **2006**, *8* (9), 1674−1679.
(58) Torres, S.; Pandey, A.; Castro, G. R. Organic solvent adaptation of Gram positive bacteria: applications and biotechnological potentials. *Biotechnol. Adv.* **2011**, *29* (4), 442−452.

(59) Nicolaou, S. a.; Gaida, S. M.; Papoutsakis, E. T. A comparative view of metabolite and substrate stress and tolerance in microbial bioprocessing: From biofuels and chemicals, to biocatalysis and bioremediation. *Metab. Eng.* **2010**, *12* (4), 307−331.
(60) Yuvaniyama, P.; Agar, J. N.; Cash, V. L.; Johnson, M. K.; Dean, D. R. NifS-directed assembly of a transient [2Fe-2S] cluster within the NifU protein. *Proc. Natl. Acad. Sci. U.S.A.* **2000**, *97* (2), 599−604.
(61) Smith, A. D.; Jameson, G. N.; Dos Santos, P. C.; Agar, J. N.; Naik, S.; Krebs, C.; Frazzon, J.; Dean, D. R.; Huynh, B. H.; Johnson, M. K. NifS-mediated assembly of [4Fe-4S] clusters in the N- and C-terminal domains of the NifU scaffold protein. *Biochemistry* **2005**, *44* (39), 12955−12969.
(62) Frees, D.; Qazi, S. N.; Hill, P. J.; Ingmer, H. Alternative roles of ClpX and ClpP in *Staphylococcus aureus* stress tolerance and virulence. *Mol. Microbiol.* **2003**, *48* (6), 1565−1578.
(63) Michel, A.; Agerer, F.; Hauck, C. R.; Herrmann, M.; Ullrich, J.; Hacker, J.; Ohlsen, K. Global regulatory impact of ClpP protease of *Staphylococcus aureus* on regulons involved in virulence, oxidative stress response, autolysis, and DNA repair. *J. Bacteriol.* **2006**, *188* (16), 5783−5796.
(64) Tomas, C. A.; Beamish, J.; Papoutsakis, E. T. Transcriptional analysis of butanol stress and tolerance in *Clostridium acetobutylicum*. *J. Bacteriol.* **2004**, *186* (7), 2006−2018.
(65) Boschi-Muller, S.; Olry, A.; Antoine, M.; Branlant, G. The enzymology and biochemistry of methionine sulfoxide reductases. *Biochim. Biophys. Acta* **2005**, *1703* (2), 231−238.
(66) Sasindran, S. J.; Saikolappan, S.; Dhandayuthapani, S. Methionine sulfoxide reductases and virulence of bacterial pathogens. *Future Microbiol.* **2007**, *2* (6), 619−630.
(67) Kumsta, C.; Jakob, U. Redox-regulated chaperones. *Biochemistry* **2009**, *48* (22), 4666−4676.
(68) Poole, L. B. Bacterial defenses against oxidants: mechanistic features of cysteine-based peroxidases and their flavoprotein reductases. *Arch. Biochem. Biophys.* **2005**, *433* (1), 240−254.
(69) Kang, I. H.; Kim, J. S.; Kim, E. J.; Lee, J. K. Cadaverine protects Vibrio vulnificus from superoxide stress. *J. Microbiol. Biotechnol.* **2007**, *17* (1), 176−179.
(70) Ha, H. C.; Sirisoma, N. S.; Kuppusamy, P.; Zweier, J. L.; Woster, P. M.; Casero, R. A. The natural polyamine spermine functions directly as a free radical scavenger. *Proc. Natl. Acad. Sci. U.S.A.* **1998**, *95* (19), 11140−11145.
(71) Brown, A. D. Inhibition by spermine of the action of a bacterial cell-wall lytic enzyme. *Biochim. Biophys. Acta* **1960**, *44* (0), 178−179.
(72) Brown, A. D.; Drummond, D. G.; North, R. J. The peripheral structures of Gram-negative bacteria: II. Membranes of bacilli and spheroplasts of a marine pseudomonad. *Biochim. Biophys. Acta* **1962**, *58* (3), 514−531.
(73) Pegg, A. E.; Michael, A. J. Spermine synthase. *Cell. Mol. Life Sci.* **2010**, *67* (1), 113−121.
(74) Joshi, G. S.; Spontak, J. S.; Klapper, D. G.; Richardson, A. R. Arginine catabolic mobile element encoded speG abrogates the unique hypersensitivity of *Staphylococcus aureus* to exogenous polyamines. *Mol. Microbiol.* **2011**, *82* (1), 9−20.
(75) Mashima, R.; Nakanishi-Ueda, T.; Yamamoto, Y. Simultaneous determination of methionine sulfoxide and methionine in blood plasma using gas chromatography-mass spectrometry. *Anal. Biochem.* **2003**, *313* (1), 28−33.
(76) Mailloux, R. J.; Singh, R.; Brewer, G.; Auger, C.; Lemire, J.; Appanna, V. D. α-Ketoglutarate Dehydrogenase and Glutamate Dehydrogenase Work in Tandem To Modulate the Antioxidant α-Ketoglutarate during Oxidative Stress in *Pseudomonas fluorescens*. *J. Bacteriol.* **2009**, *191* (12), 3804−3810.
(77) Mailloux, R. J.; Beriault, R.; Lemire, J.; Singh, R.; Chenier, D. R.; Hamel, R. D.; Appanna, V. D. The tricarboxylic acid cycle, an ancient metabolic network with a novel twist. *PLoS One* **2007**, *2* (8), e690.